Electron Accelerators Driven by Modulated Intense Relativistic Electron Beams

M. Friedman, V. Serlin, Y. Y. Lau, and J. Krall
Plasma Physics Division, Naval Research Laboratory, Washington, D.C. 20375-5000
(Received 17 July 1989)

This paper addresses the development of a new high-voltage-gradient linear accelerator. This accelerator was energized by a modulated intense relativistic electron beam with power in the multigigawatt range. A 0.2-cm-diam electron beam emerged from the accelerator with a peak current of ~ 200 A and peak kinetic energy ≥ 60 MeV. The length of the accelerating structure was 1 m. Simple scaling laws suggest that similar accelerators with much higher average electric fields can be built.

PACS numbers: 41.80.Ee, 29.15.Dt

Mechanisms that can establish high voltage gradients in accelerating structures have been the subject of many papers and conferences.[1] In one class of acceleration mechanisms, there are two beams of particles traveling through a structure. The first beam (labeled beam 1) leaves behind an electromagnetic field. The second beam (labeled beam 2) is accelerated by this electromagnetic field. The effect is large only when the second beam is much weaker and/or shorter in duration than the first. The two beams are coupled electromagnetically to each other by a metallic structure which can be viewed as a transformer. We at NRL pioneered this research in the 1970s in what was called "autoacceleration" of intense relativistic electron beams.[2,3] In that research, part of an intense relativistic electron beam (beam 1) induced an electric field in cavities which were inserted in a drift tube. The electric field interacted in turn with a subsequent portion of the same electron beam (beam 2) causing acceleration of electrons. Experiments were successful, for example, accelerating a beam of electrons with current of 70 kA to an energy of 7 MeV.[4] It was found that autoacceleration mechanisms are not scalable to higher energy for many reasons, e.g., the onset of beam instability that results from the common trajectory shared by the intense relativistic electron beam and the accelerated beam.

New ideas for acceleration of electrons or ions by a driving electron beam with a modulated current profile were suggested in the last few years.[5,6] Here the driving electron beam and the accelerated beam can exchange energy while moving on different trajectories. The new mechanisms are scalable and can lead to generation of high-energy particle beams. One of these mechanisms is currently under investigation at NRL. Here,[7] the driving beam is a modulated intense relativistic electron beam (MIREB) which transfers energy through an appropriate structure to a secondary electron beam. The two beams share different parts of the same structure.

The generation of a MIREB, using an external rf source, was discussed previously.[8,9] This MIREB consisted of a train of electron bunches which were phase locked to the external rf source to better than 4°. The electron bunches were annular in shape with a diameter of 13.2 cm, thickness of 0.3 cm, and lasted for a period of ~ 100 nsec. The current profile of the MIREB used in the experiment was

$$I=\sum_{n=0} I_n \cos(n\omega t), \quad f=\omega/2\pi=1.3\ \text{GHz}, \tag{1}$$

where $I_0=16$ kA, $I_1=12$ kA, and $I_2, I_3, \ldots, I_n < I_1$. The kinetic energy of the electrons was ~ 600 keV.

The experimental setup that was used to investigate the acceleration mechanism is shown in Fig. 1. It consisted of a high-voltage gap across which the MIREB propagated. The gap fed a coaxial transmission line that was connected to an rf structure via coupling loops.

The input impedance of the gap, Z, was controlled by a plunger in the coaxial line and by the shape and number of the coupling loops. By a proper choice of these parameters Z became real ($=R$) at the frequency of modulation ($f=1.3$ GHz) and a voltage $V_1=RI_1$ was developed across the gap. V_1 and I_1 were in phase, and hence energy was drawn from the MIREB and transferred to the structure. The rf structure[7] consisted of a cylindrical metallic shell, 22.8 cm in diameter. Arranged coaxially inside the shell were 54 thin metallic disks, 17.95 cm in diameter. The disks were evenly spaced in such a way that every six occupied a length equal to $\lambda/2=f/2c$. The 54 disks were supported by longitudinal and radial thin metallic rods. This structure was designed using the SUPERFISH[10] computer code. It supported an axially symmetric accelerating rf wave of frequency $f=1.3$ GHz with a phase velocity $v_f=c$. The supporting rods were positioned at the zero-electric-field points. A metallic pin of radius $r_p=1$ mm placed at one end of the rf structure served as a field-emission cathode. The pin was located on axis at a maximum-electric-field point and was aligned with a small hole of radius 5 mm at the center of each disk, allowing complete transmission of the beam.

The experiment was evacuated to a base pressure of $\sim 10^{-5}$ Torr using an oil diffusion pump. In contrast to conventional accelerator systems no special care was taken to get a better vacuum and/or a hydrocarbon-free en-

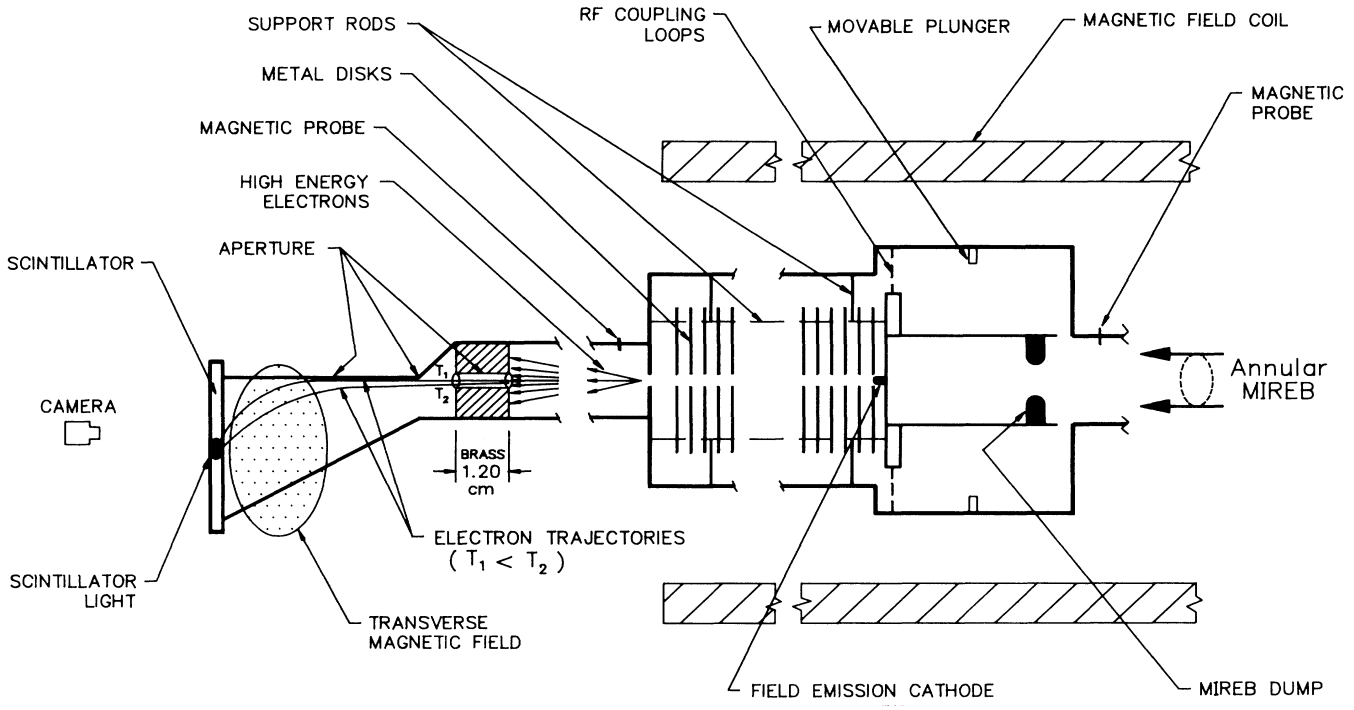

FIG. 1. Accelerating structure with particle energy analyzer.

vironment. A uniform quasi dc axial magnetic field ($B_0=10$ kG) was imposed on the structure. The Q of the rf-structure–coaxial-line combination at $f=1.3$ GHz was $Q\geq 2000$.

In the experiment the input impedance of the gap, R, was adjusted such that rf power of ~ 3 GW was transferred to the structure.[11] The peak rf voltage that appeared on the gap was $V_1=2P/I_1\sim 500$ kV. The 3-GW rf power was pumped into the accelerating structure for a duration of 100 nsec. 30 nsec into the duration of the pulse the pin cathode started to emit electrons. The electrons were focused by the dc magnetic field and propagated through the structure. Figure 2 gives the input MIREB current and the current from the pin cathode. The peak current was ~ 200 A. The size of this beam was determined from the damage it inflicted on witness plates constructed of Lucite or lead. The witness plates were located inside or outside the magnetic field coil ($B_0=0.5$ kG at the outside position). A 2-mm-diam "crater" was detected on each of the witness plates. When a Lucite block was used to terminate the electron beam, a "linac tree" a few centimeters in length was established after a few pulses. There was no evidence of electron loss during the acceleration process as the crater dimensions matched those of the pin cathode.

The kinetic energy of the electrons was measured after extracting the beam into a magnetic-field-free region. While doing so, some important results were obtained.

We found that electrons gain perpendicular velocity v while propagating into a magnetic-field-free region. This is an intrinsic velocity that originates from conservation of canonical angular momentum:

$$\frac{v}{c}=\frac{1}{2}\frac{eB_0}{\gamma mc}\left[\frac{r_0^2}{r}\right], \tag{2}$$

where $r_0=r_p$ is the radius of the beam at the pin cathode, $B_0=10$ kG, and r is the radius of the beam at a position at which the axial magnetic field intensity is $\ll B_0$ (e.g., outside the magnetic field coil). Propagating the beam a distance $l_b=100$ cm in an evacuated drift tube located in the magnetic-field-free region resulted in a radial expansion of the beam to a radius $r_b=1$ cm. Hence

$$v/c=r_b/l_b=0.01\,. \tag{3}$$

Since $r_0\simeq r\simeq 1$ mm one gets from Eqs. (2) and (3) that the minimum energy of the electrons must be ≥ 15 MeV. Note that the preceding estimate assumes zero beam emittance. Inclusion of finite emittance requires a minimum energy higher than 15 MeV to account for beam spreading in vacuum.

A different kind of radial expansion of the electron beam occurred when the magnetic-field-free region was filled with air at atmospheric pressure. Here, the electron beam propagated a distance of $l_b^*=0.6$ m and expanded radially to $r_b^*=1.5$ cm. The square of the angle of scattering of electrons with an energy T (in MeV) after propagation over a distance l_b^* in atmospheric air

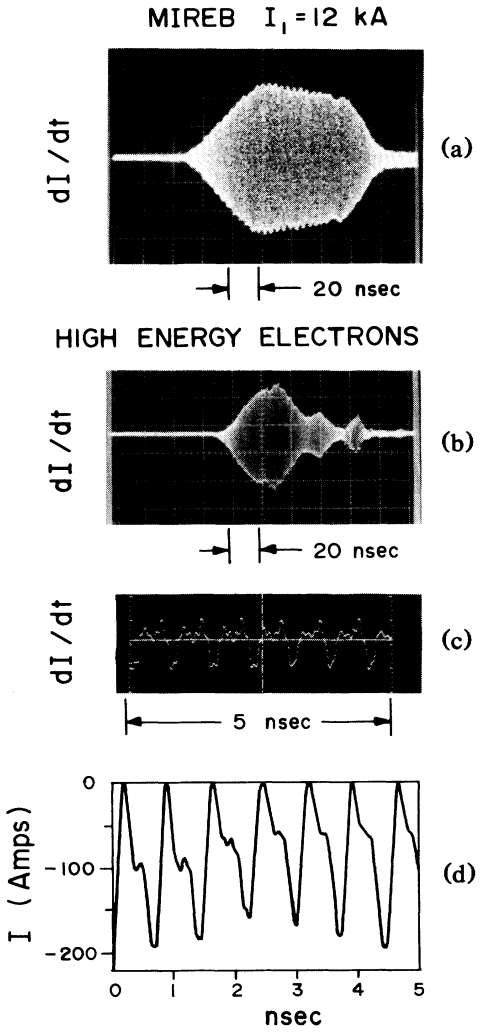

FIG. 2. Magnetic probe signals for (a) MIREB, (b) accelerated electrons as measured by a 1-GHz Tektronix R7103 oscilloscope, (c) expanded time window of (b) as measured by a 6-GHz Tektronix 7250 oscilloscope, and (d) electron current derived from (c) by numerical integration.

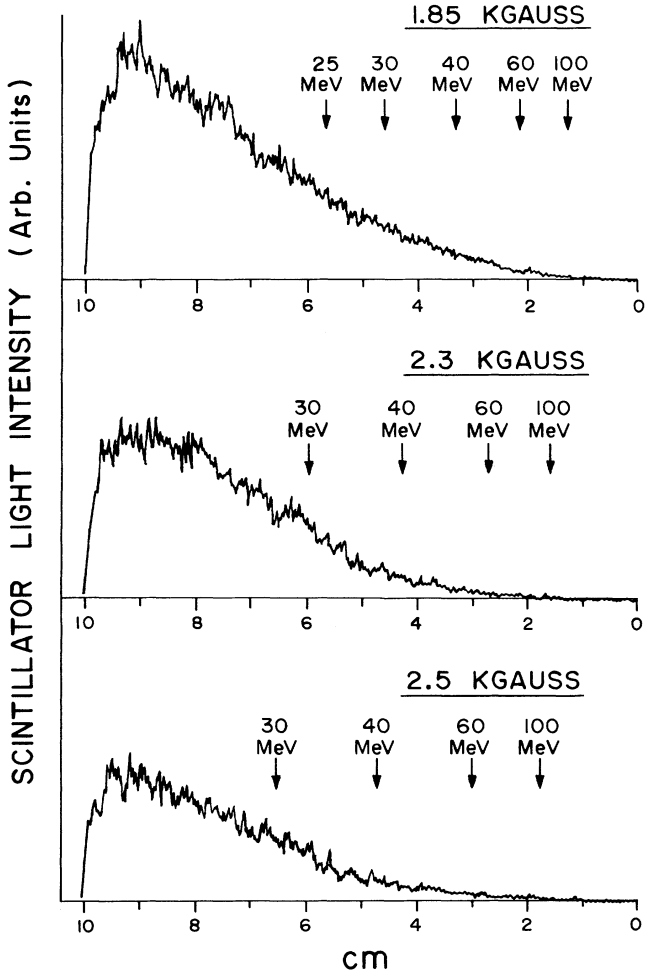

FIG. 3. Scintillator light intensity as a function of position and of magnetic field intensity. Arrows (with energy labels) point to positions where electrons with energies equal to or greater than the label energies strike the scintillator.

is[12]

$$\langle\theta^2\rangle_{\rm av}=\left[\frac{21}{T}\right]^2\left[\frac{l_b^*}{300}\right]. \tag{4}$$

Since

$$\langle\theta^2\rangle_{\rm av}^{1/2}=r_b^*/l_b^*,$$

one gets $T=40$ MeV. This is again a lower limit on the beam energy since we did not include other effects, such as the radial velocity of Eq. (2), scattering from the exit foil, etc.

The kinetic energy of the electrons was determined using a magnetic "spectrograph." This measuring device was placed in the magnetic-field-free region and consisted of an evacuated drift region, part of which was located between the two poles of an electromagnet. A set of apertures selected electrons with predetermined initial parameters. These electrons were deflected by the transverse magnetic field. The angle of deflection was calculated from the impact point of the electrons on a plastic scintillator. The light that emerged from the impact point was detected photographically.

We found that the intrinsic radial velocities of the electrons [Eq. (3)] smeared the apparent energy distribution of the electrons as obtained by the spectrograph. Using apertures to eliminate electrons with large radial velocities failed, since it resulted in an increase in the background noise of x rays and secondary and scattered electrons. The spectrograph was useful, however, in that we were able to obtain a lower limit on the maximum energy of the electrons.

A thick obstacle was used to eliminate half of the electrons [those moving above (or below) the horizontal

plane defined by the axis of the rf structure and the direction of the deflecting magnetic field]. The transverse magnetic field was chosen such that the trajectories of the electrons entering the spectrograph were directed away from the (above mentioned) horizontal plane as in Fig. 1. Under these conditions, a spot of light at a given point on the scintillator originated from electrons with wide energy and radial velocity distributions. Electrons that enter the spectrograph with trajectories along the axis had zero radial velocity and kinetic energy T_1 (see Fig. 1). This energy is easily calculated from the geometry and the transverse magnetic field intensity. An electron that entered with a nonzero radial velocity or with a trajectory that was not coincident with the axis had energy $T_2 > T_1$ (see Fig. 1). By measuring the position of a spot of light on the scintillator, one can calculate the minimum energy of the electrons that terminated at that spot ($=T_1$).

Figure 3 shows a densitometer scan of several photographs of the scintillator taken for various transverse magnetic field intensities. Using these figures a *lower* limit of the maximum electron kinetic energy was established:

$$T \geq 60 \text{ MeV}.$$

We now speculate on the impact of these results on future accelerators. We believe that a similar accelerating structure with an average electric field of > 200 MV/m can be built, for the following reasons.

(1) The accelerating structure of the present experiment has an average electric field of the order of 60 MV/m and peak electric field of the order of 120 MV/m. By rearranging the distances between the disks in the structure the average electric field can be increased by at least 50%, to 90 MV/m.

(2) The MIREB power can be increased by a factor of 10 resulting in an increase in the average electric field by a factor of 3.

(3) Using a MIREB of higher frequency can increase the electric field intensity (e.g., a factor of 2 for 5-GHz modulation).

Eventually vacuum breakdown will limit the electric field inside the structure. Reducing the probability of vacuum breakdown in the present experiment can be easily achieved by adopting the clean environment associated with conventional accelerators. Most of the above suggestions will be implemented in a future experiment.

In addition, one can look at this device as a single stage of a multistage accelerator. The proper phasing of the driving MIREB's can be accomplished using a master rf generator that phase locks each of the MIREB's so as to achieve optimum acceleration.

This work is supported by the Department of Energy, under Contract No. DE-AI05-86 ER 13585.

[1]For example, see *Advanced Accelerator Concepts,* edited by C. Goshi, AIP Conference Proceedings No. 193 (American Institute of Physics, New York, 1989).

[2]M. Friedman, Phys. Rev. Lett. **32**, 92 (1974).

[3]T. R. Lockner and M. Friedman, J. Appl. Phys. **51**, 6068 (1981).

[4]M. Friedman, Appl. Phys. Lett. **41**, 419 (1982).

[5]G. Voss and T. Weiland, DESY Report No. M82-10, 1982 (unpublished).

[6]D. B. Hopkins *et al.*, in *Advanced Accelerator Concepts,* edited by C. Goshi, AIP Conference Proceedings No. 193 (American Institute of Physics, New York, 1989).

[7]M. Friedman and V. Serlin, Appl. Phys. Lett. **49**, 596 (1986).

[8]M. Friedman and V. Serlin, Phys. Rev. Lett. **55**, 2860 (1985).

[9]M. Friedman, J. Krall, Y. Y. Lau, and V. Serlin, J. Appl. Phys. **64**, 3353 (1988).

[10]K. H. Halbach and R. F. Holsinger, Lawrence Berkeley Laboratory Report No. LBL-5040, 1976 (unpublished).

[11]M. Friedman, J. Krall, Y. Y. Lau, and V. Serlin, Rev. Sci. Instrum. (to be published); Proc. SPIE **1061**, 34 (1989).

[12]See, for example, B. Rossi, *High-Energy Particles* (Prentice-Hall, New York, 1952).

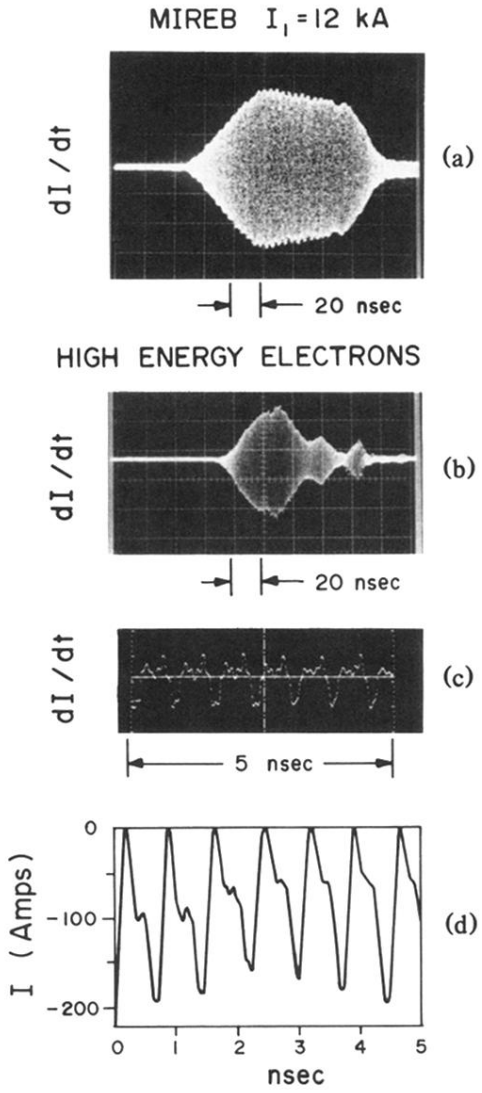

FIG. 2. Magnetic probe signals for (a) MIREB, (b) accelerated electrons as measured by a 1-GHz Tektronix R7103 oscilloscope, (c) expanded time window of (b) as measured by a 6-GHz Tektronix 7250 oscilloscope, and (d) electron current derived from (c) by numerical integration.